RAA 2016 Vol. **16** No. **6**, 88 (8pp) doi: 10.1088/1674–4527/16/6/088
http://www.raa-journal.org *http://iopscience.iop.org/raa*

Research in Astronomy and Astrophysics

A substorm-associated enhancement in the XUV radiation measuring channel observed by ESP/EVE/*SDO*

Yan Yan[1,2,4], Hua-Ning Wang[1,2], Chao Shen[3] and Zhan-Le Du[1,2]

[1] National Astronomical Observatories, Chinese Academy of Sciences, Beijing 100012, China; *yyan@bao.ac.cn*
[2] Key Laboratory of Solar Activity, Chinese Academy of Sciences, Beijing 100012, China
[3] School of Natural Sciences and Humanity, Harbin Institute of Technology Shenzhen Graduate School, Shenzhen 518055, China
[4] University of Chinese Academy of Sciences, Beijing 100049, China

Received 2014 April 7; accepted 2015 December 1

Abstract Comparing the ESP/EVE/*SDO* flux data of 2011 Feb 6, with the counterparts of XRS/*GOES* and SEM/*SOHO*, we find that there is an enhancement that is not apparent in the two latter datasets. The enhancement, possibly regarded as a flare at first glimpse, nevertheless, does not involve an energy-release from the Sun. Based on the enhancement, we combine data from SXI/*GOES* 15 into a synthesized analysis, and concluded that it arises from a particle-associated enhancement in the channel that measures XUV radiation. Paradoxically, it seems to be somewhat of a particle-avalanching process. Prior to the event, a moderate geomagnetic storm took place. Subsequently, while the event is proceeding, a geomagnetic substorm is simultaneously observed. Therefore, the particles, though unidentified, are probably energetic electrons induced by substorm injection.

Key words: Sun: X-rays, gamma rays — Sun: flares — Sun: solar-terrestrial relations

1 INTRODUCTION

Solar irradiance had been studied for a very long time, nearly throughout the entire history of astronomy, from ancient times in optical, to modern times, extending longward to radio, and shortward to ultraviolet, X-ray and even γ ray. The ultraviolet irradiance, an important parameter in the field of space weather, however, was less studied until humans entered the space age. Originally, the observational data were less reliable, often discontinuous, and confined to being acquired from equipment carried by balloons or rockets (Lean 1987). After that, several spacecrafts were launched into space and solar astronomers began to, systematically say, pay more and more attention to the irradiance range of Extreme UltraViolet (hereafter EUV) and Soft X-ray (hereafter XUV). What we primarily focus on here is the so-called "XUV," the electromagnetic wave with a wavelength ranging from 0.1 to 10 nm, the most sensitive one for tracking solar eruptions.

It is generally recognized that XUV irradiance can be the most effective tracer of solar flares. In order to surveil them in realtime, members of the *Geostationary Operational Environment Satellite* (hereafter *GOES*) series were successionally sent into geostationary orbit, from 1974 (Grubb 1975) until today. Currently, GOES 15 is in operation, and has been the primary satellite used for this purpose. It is equipped with the solar X-Ray Sensor (hereafter XRS), the Soft X-ray Imager (hereafter SXI) and other instruments. More recently, launched into space on 2010 Feb 11, the *Solar Dynamics Observatory* (hereafter *SDO*) (Pesnell et al. 2012), the first instrument of NASA's Living With a Star Program, helps us unveil both characteristics of the Sun's interior and its exterior influence on the Earth and its nearby space. The Extreme Ultraviolet Variability Experiment (hereafter EVE) (Woods et al. 2012) onboard *SDO* measures the EUV irradiance of the Sun from 0.1 to 105 nm, including the Multiple EUV Grating Spectrographs and EUV SpectroPhotometer (hereafter ESP) (Didkovsky et al. 2012), a broadband spectrograph. In addition, the Solar EUV Monitor (hereafter SEM) onboard the Solar and Heliospheric Observatory (hereafter *SOHO*) (Judge et al. 1998), has the highest temporal resolution of 0.25 second, currently the best available. ESP has two orders: the first order covers four channels of 18.2, 25.7, 30.4 and 36.6 nm in measuring the line intensity of four spectral lines, whereas, the zeroth one covers the broadband between 0.1 and 7 nm, primarily for space weather. Fruitful results have been published in articles about ESP/EVE. Didkovsky et al. (2011) discovered 5-min oscillations in the corona and Didkovsky et al. (2013) further found related variability. Both papers discussed how the EUV/XUV radiation is directly relevant to the Sun. Most researchers in the space weather community considered the fluctuations of XUV radiation to be solar flares as well, and Du & Wang (2012) gave a tentative relationship of solar flares with both sunspot and geomagnetic activity. This study examines an unusual enhancement observed by ESP/EVE/*SDO*. By analyzing dozens of imaging data sets from SXI/*GOES* 15 together, we will highlight a counterexample which is not a solar flare, but is rather a substorm-associated enhancement. Section 2 describes observations in detail and provides a comparison of the data and associated analysis. Finally, summary and discussion are discussed in Section 3.

2 OBSERVATIONS AND DATA

Three soft X-ray light curves representing flux data on 2011 February 6 are introduced, see Figure 1. Figure 1(a) was recorded by XRS/*GOES* 15 over 24 hours in the 0.1–0.8 nm wavelength band; Figure 1(b) was from ESP/EVE/*SDO* covering the broader wavelength band of 0.1–7 nm; Figure 1(c) was acquired by SEM/SOHO. A comparison will be discussed later. Besides the flux data, we also consider dozens of images obtained by SXI (Hill et al. 2005; Pizzo et al. 2005) onboard *GOES* 15 to see what transpired in the meantime. The images are all level-1 FITS data with the filter of BEA covering the spectral band pass of 0.6–1.2 nm. Their exposure time is approximately 1 s.

2011 February 6 was indeed a calm day in terms of solar activity. Only two active regions (ARs) appeared on the solar disk, NOAA AR 11152 and AR 11153, both of which stayed quiet throughout the 24 hours. These ARs showed simple magnetic configurations and the area of their associated sunspots were small as summarized by the Space Weather Prediction Center. A *GOES* soft X-ray flux diagram is plotted as Figure 1(a). From the plot, one can clearly learn that no flare happened, even in B class. Analogously, ESP is another instrument that can measure soft X-ray flux with higher cadence. We survey ESP zeroth order data in the same interval as XRS and find something different which is not displayed in the plot of XRS. As shown in Figure 1(b), a remarkable increase that appears as a burst is shown in this plot. This strongly resembles a solar flare in both shape and duration. The main phase of the event, beginning at about 08:48 UT, afterwards, shows a fast upsurge. It peaks at 09:18 UT, with a flux of 2.7×10^{-4} W m^{-2}. The relative increment almost reaches 40% compared with the background flux. The phase lasts almost 100 min and behaves like a solar-flare, whose main features are listed in Table 1.

Whether this event is a true flare or not perplexed us. We scrutinized the SEM/SOHO data up at the corresponding time to further analyze this event. The result plotted in Figure 1(c) does not exhibit any notable increase. *SDO* is in a geosynchronous orbit whereas SOHO is located near L1 which is far from Earth. Therefore, the enhancement observed by ESP/EVE is possibly not associated with the Sun, but rather operating in space near the Earth (Didkovsky L. 2012b, private communication).

Didkovsky et al. (2012) has clearly stated that it is possible to use the $C_{\rm dark}$ measurements (available at any time) as a proxy for dark counts in the science bands, and as a proxy for particle-background signal. In view of this statement, we have checked the simultaneous data in the dark band, which is completely closed at all times, as seen in Figure 2. From the figure, we can see that the $C_{\rm dark}$ channel also exhibits a peak that coincides in terms of time. This suggests to us that the $C_{\rm dark}$ peak has a certain connection with the counterpart appearing in the XUV channel. The absolute scale of the ESP zeroth order and $C_{\rm dark}$ channel is different because of their different sensitivities to particle contamination.

For clarifying what really happened during this event, we further examine the data from SXI. Also onboard *GOES*, SXI is responsible for imaging the Sun in soft X-ray wavelengths, overlapping with the wavelengths covered by ESP. We select the data which cover the period of the event and carefully check them with image processing. Twenty-four images in total from 08:00 UT to 11:04 UT taken with an 8 minute cadence are investigated, all of which are in 580×512 pixels. We extracted 406×406-pixel images, and coaligned them to the first image taken at 08:00 UT, which is shown in Figure 3(a). Since 08:48 UT, unexpected dazzling specks quickly appeared on the images. In addition, the amount of specks on each image is beginning to increase rapidly.

In Figure 3(c), the largest amount of the specks show up near the peak. For interpreting this more clearly, we identified various parts of the images. The clustered, brilliant areas represent the intense XUV regions (hereafter XIR) on the Sun, whereas the scattered bright specks are unrelated. We mark the XIR alphabetically, see Figure 3. Regions A, B, C and D are all XIR, however, Region E is void of any XUV blocks, but numerous specks are seen.

Afterwards, for the sake of quantitatively comparing the images with the flux plot from ESP, we extract different rectangular regions and independently integrate them. The results are itemized in Table 2. This table lists the result of integration of the full disk as well. In the column labeled full disk, we can decern that the value in the row of 09:20 UT is the maximum around the time interval, according to the peak time in Figure 1(b).

Figure 4 plots the relative increment of integrated DN of the selected regions in Figure 3, according to the formula

$$\Delta DN_r(\%) = \frac{DN_i - DN_1}{DN_1} \times 100\% \quad (i = 1 \cdots 24), \qquad (1)$$

where ΔDN_r means relative increment, and DN_i represents the DN integral of each region in each image. This reflects the trends demonstrating the relative increment in the corresponding region in Figure 3 in the time interval. It is worth noting that all XIR are descending just at the time the peak happens. Hence, there should be an external cause driving the climb in total flux. Consequently, there is a rapid rise in the specks. Region E, a void of XUV radiation, disagrees with the XIR. Also, the result of Region E,

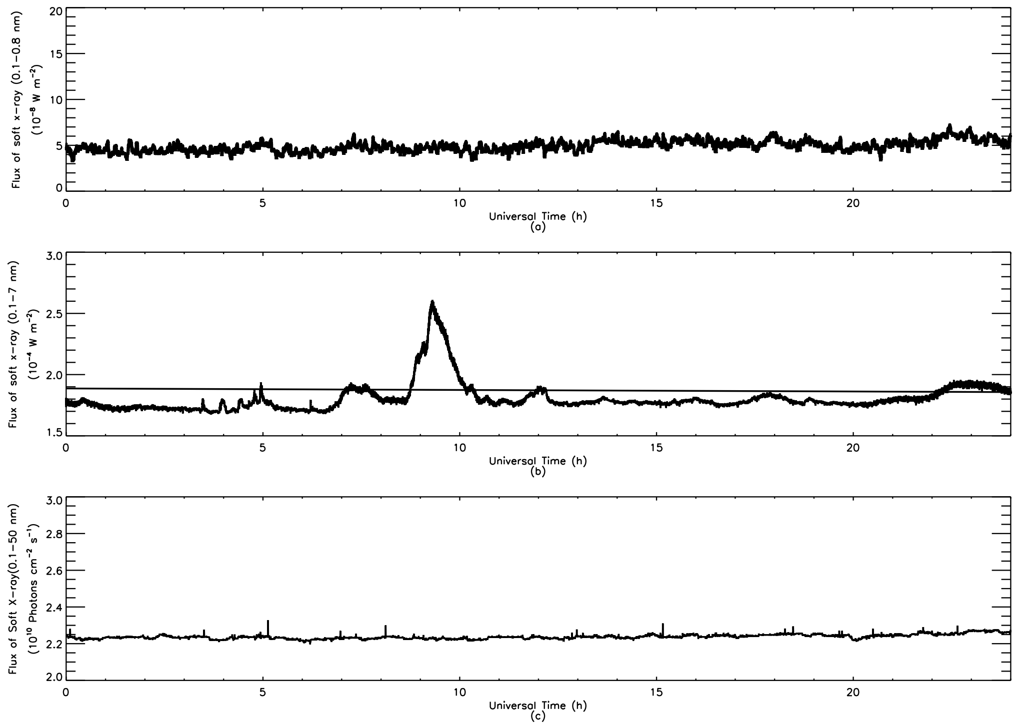

Fig. 1 Time-intensity profiles of three monitors on 2011 February 6. (a) 0.1–0.8 nm XUV variation from XRS/*GOES* 15, (b) 0.1–7 nm XUV variation from ESP/EVE/*SDO*, (c) 0.1–50 nm XUV/EUV variation from SEM/*SOHO*.

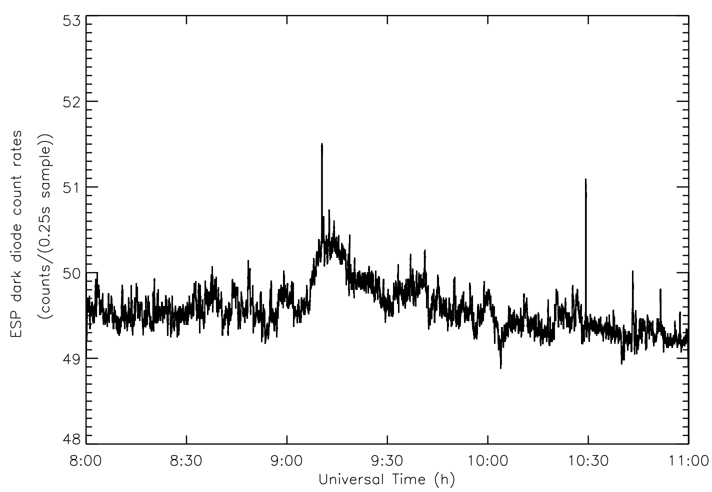

Fig. 2 Time profile of the dark band counts from UTC 8:00 to 11:00 on 2011 Feb 6. The profile is shown with a 10-s smoothing window.

Table 1 Parameters of the Unusual Enhancement

Start time	Peak time	End time	Duration	Peak flux	Relative increment
08:48	09:18	10:20	90 min	2.7×10^{-4} Wm^{-2}	40%

shown in Figure 4, as we expect, coincides with the shape of the light curve of Figure 1(b), confirming that the two plots have a strong relationship in terms of time correspondence, although the two corresponding flux values may not be equivalent. The reason for the different amplitudes of the fluxes was perhaps that the two instruments were in different astronomical positions, had different angles of view, and the event itself had its own angular distribution. By quantitative image analysis, we confirm that the flare-like enhancement is not attributed to the Sun, but rather is a cumulative effect of the speckles spreading all over the images.

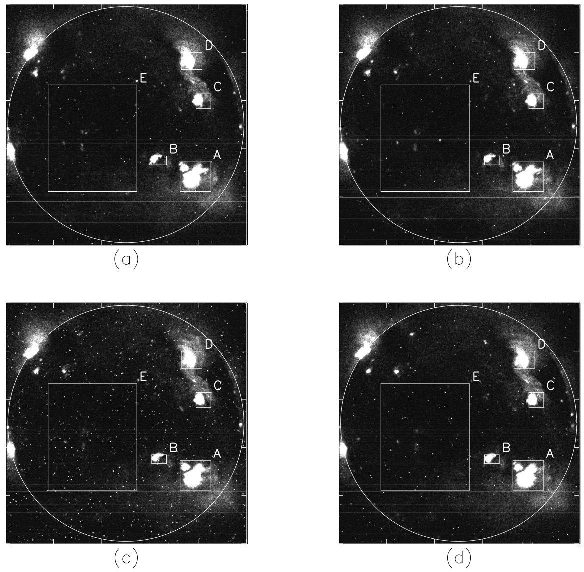

Fig. 3 Selected regions in the 406×406-pixel images taken by SXI/*GOES* 15 at 08:00 UT(a), 08:48 UT(b), 09:20 UT(c) and 10:24 UT(d), on 2011 February 6. Five different regions are marked alphabetically in each image. Regions A, B, C and D are all XIR, whereas Region E is void of XUV radiation.

Table 2 Integrated DN of the Selected Regions in Each Image

Time	Region A	Region B	Region C	Region D	Full Disk	Region E
08:00	399393	45872	89658	114929	2444431	179517
08:08	394135	46327	98044	109796	2471575	178751
08:16	394297	46311	105509	105177	2479881	180469
08:24	392344	45795	105719	102841	2448795	179467
08:32	397577	41153	107416	100966	2442060	184668
08:40	397890	39205	103751	97561	2427595	182135
08:48	402903	37953	99987	97910	2414410	181976
08:56	403556	35768	100816	95671	2425859	183018
09:04	398969	40411	95974	96707	2437488	188256
09:12	394309	38111	87636	97508	2472689	193812
09:20	378964	38745	85754	94270	2475250	197167
09:28	372735	37891	95094	95003	2455289	196342
09:36	363798	39524	104259	92438	2439830	189023
09:44	368264	42317	103760	93148	2414413	189696
09:52	363344	40725	100012	91797	2414680	185804
10:00	366945	38536	103437	91695	2401754	193474
10:08	365885	38438	102047	90118	2381712	181975
10:16	363385	45572	104163	90209	2395087	181770
10:24	360601	48509	107047	93240	2399176	179427
10:32	365307	54978	105312	90738	2389448	183443
10:40	371526	53237	103746	90381	2397264	185767
10:48	373265	51628	98713	89235	2403487	187137
10:56	382002	47589	97935	89631	2417106	185402
11:04	381363	51194	98402	90643	2468105	182755

What the speckles are should be a very interesting question that can perhaps open new lines of research. Naturally, geosynchronous relativistic electron enhancement (hereafter GREE) is a feasible consideration relating to the event. GREEs mostly have a strong connection with geomagnetic activity. A moderate geomagnetic storm took place with a minimum Dst index of –63 nT on UTC 22:00 Feb 4, and lasted at least six days, from the beginning phase to the recovery phase. The time of the event was during the recovery phase of the magnetic storm, while the magnetic field is still active, as Figure 5 shows. Separate from the magnetic storm, the speed of the solar wind stream goes up to a large value, with a maximum of 670 km s^{-1}, which is maintained for a rather long time (almost 50 hours or more) with a speed higher than 500 km s^{-1}. Rathore et al. (2015) highlighted the im-

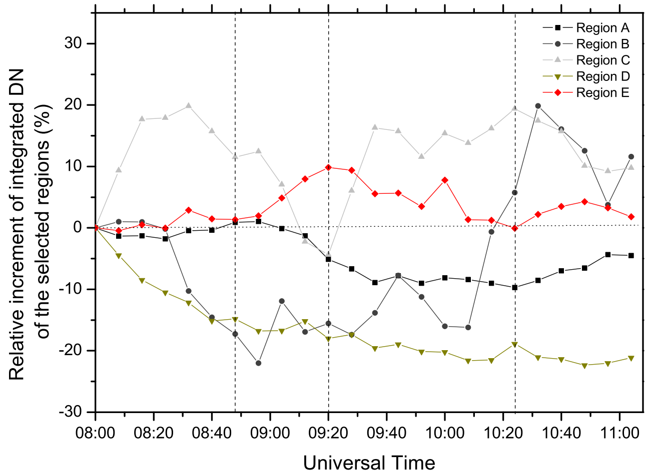

Fig. 4 Plots of the relative increment of integrated DN for the selected regions. We take the values at 08:00 UT as the initial values, and other values are calculated from Eq. (1). Three reference lines (*dashed lines*) are marked to represent the start time, peak time and end time, from left to right respectively.

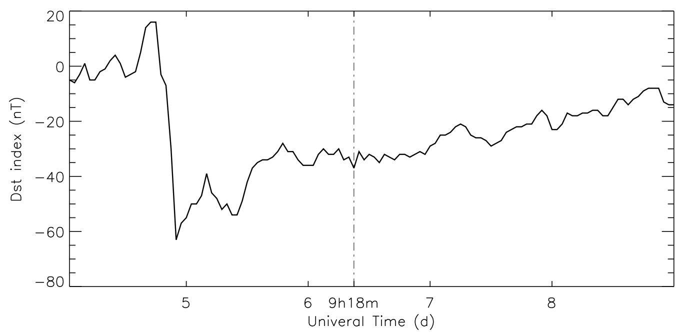

Fig. 5 Hourly Dst index from 2011 Feb 4 to 2011 Feb 9, adapted from WDC for Geomagnetism, Kyoto. A moderate geomagnetic storm has taken place, with the minimum Dst index of −63 nT.

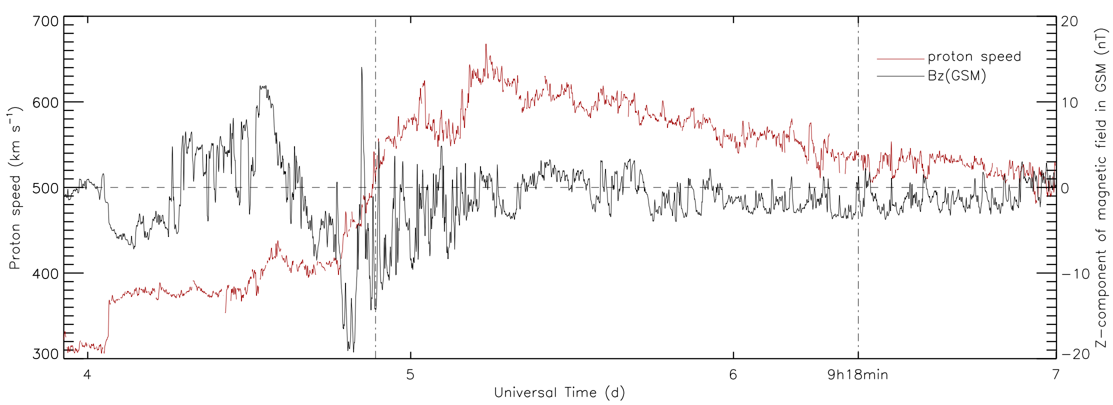

Fig. 6 Time profiles of one-minute proton speed and the z component of magnetic field in GSM from 2011 Feb 4 to Feb 7, adapted from WDC for Geomagnetism, Kyoto. The proton speed (*red line*) reflects the solar wind speed, whereas the z component of magnetic field in GSM (*black line*) traces the z component of the IMF. The left vertical dot-dashed line refers to the onset of the magnetic storm, whereas the right one indicates the peak of the enhancement.

portance of solar wind parameters in space weather, two of which were the solar wind speed and the southward component of the Interplanetary Magnetic Field (hereafter IMF).

Figure 6 not only demonstrates the situation of the solar wind stream, but also, more appealingly, conveys the message to us that within the days during the magnetic storm, the IMF is always pointing negative, indicating that the southward component has risen. The deep depression of the plot shown in Figure 6 implicates the culprit that is responsible for the geomagnetic storm, however, other drops with duration of more than three hours though with less strength will, with high probability, develop geomagnetic substorms.

A substorm, the other fundamental magnetospheric process, unlike a geomagnetic storm, is a frequent occurrence, almost daily in the magnetosphere, with shorter timescales, often 2–3 hours. These processes always manifest colorful observational phenomena, making them hard to classify. In addition, the relationship between a geomagnetic storm and a substorm is also an ongoing debate, however, some evidence shows that substorms become more frequent during a geomagnetic storm, especially during its recovery phase, while the southward IMF still continues. In this case, we have examined the one-minute data of AE, AU, AL and AO indices at the right time when the event is ongoing.

As can be seen in Figure 7, a classical substorm is being measured on the timescale that is used. The AE index, an indicator of the substorm, climbs up at 904 nT and the peak time happens along the peak of the enhancement. Still, the time profile of the substorm coincides with the enhancement. On account of the geophysical conditions, GREEs are expected to occur in the outer radiation belt, about 6.6 R⊕. This evidence supports our initial speculation that the enhancement arises not from the Sun, but from a geophysical event, probably a substorm accelerating electrons into an energetic state which triggers the XUV signal.

Furthermore, we examine the electron fluxes observed by the MAGnetospheric Electron Detector (hereafter MAGED) onboard *GOES* 15, in order to examine what happened at that time. MAGED is an instrument suite, consisting of nine telescopes covering nine different directions, each with five electron energy channels from 30 keV to 600 keV. We select data to have a consistent timescale, UTC 08:00 to 11:00, and the plotted result is shown in Figure 8. The five curves respectively indicate the omni-directional electron flux with the energy channels of 40, 75, 150, 275 and 475 keV respectively, as the caption notes. From the figure, we can surmise that there are still peaks along the timescale, and the peak amplitude appears to cover the middle part of the energy range. This indicates that the electron fluxes with energy channels from 75 keV to 275 keV, especially in 150 keV, may constitute the major contribution to the enhancement observed by ESP. Substorms often introduce the so-called substorm-injection, rapidly increasing in the form of tens to hundreds of keV electrons in nearby space, and the injection in this case exhibits dispersion due to their being out of synchronization with the rise in electron flux in different energy channels. That is to say, the more energetic electrons arrive at the synchronous orbit earlier than the less energetic ones. Thanks to the enhancement observed by ESP, multi-instrument observations are accessible and a cross-match of the space physics event can therefore be carried out.

From Figure 8, it is clearly seen that the earliest arrival time of the rise in flux is after 9:00 UT, around 9:06 UT, whereas the enhancement observed by ESP began at 8:48 UT, about a quarter-hour before the former. *SDO* and *GOES* 15 are both synchronous satellites, but they are placed at two different longitudes, $102°$W and $89.5°$W, and operate almost one magnetic local time apart. The injection may have occurred as a burst at midnight, on the west of the two instruments, and diffused eastward from *SDO* to *GOES* 15. The angular velocity of the eastward propagation is estimated to be approximately $12°/18$ min or $40'$/min.

3 SUMMARY AND DISCUSSION

ESP/EVE/*SDO* record an enhancement in the XUV radiation channel in the band of 0.1–7 nm which the zeroth order data cover. In addition, there is not a remarkable surge at the corresponding time in the light curves of both XRS/*GOES* and SEM/SOHO. We then examine some relevant images taken from SXI/*GOES* 15, and are aware that the contribution of the speckles in the images are a marker of the enhancement. When we dissect the images into parts and integrate them individually, a strong time-correspondence relationship between the enhancement and the amount of the speckles is unveiled.

This instance that we encounter is scarce or accidental, because some requirements must be satisfied at the same time. When the Sun becomes inactive, the signal enhancement in the XUV observing channel might be prominent compared to the background noise, and should be detected in time. Besides this case, other similar cases should be further confirmed in the future. If they turn out to be true, we would hope to study the relationship of the flux intensity and the geomagnetic index.

Observed energetic particles detected from geosynchronous orbit are believed to have a variety of components. They are protons, electrons, α particles, heavy ions and some peculiar particles that are not always present. They have different origins which are difficult to identify. It is not easy to say from where they come. However, we can view the flux diagrams of energetic particles recorded in geosynchronous orbit to determine whether the particles have a solar origin or not. The particles are unlikely to be protons because neither a major solar eruption took place in the intervening time nor was a solar energetic proton event recorded. Moreover, they are not very heavy ions due to the great amount of the speckles. A reasonable explanation may be that they are energetic electrons. Still, they are not energetic electrons accelerated by an impulsive solar event, because the two active regions do not seem to be consistent with the coronal magnetic topology that Li et al. (2013) proposed.

One day before the event, or 2011 February 5, the solar wind speeded up to 670 km s^{-1}, injecting much more kinetic energy into the magnetosphere. As a result, the supersaturated magnetosphere would have transferred the redundant energy to the electrons nearby the magnetotail by

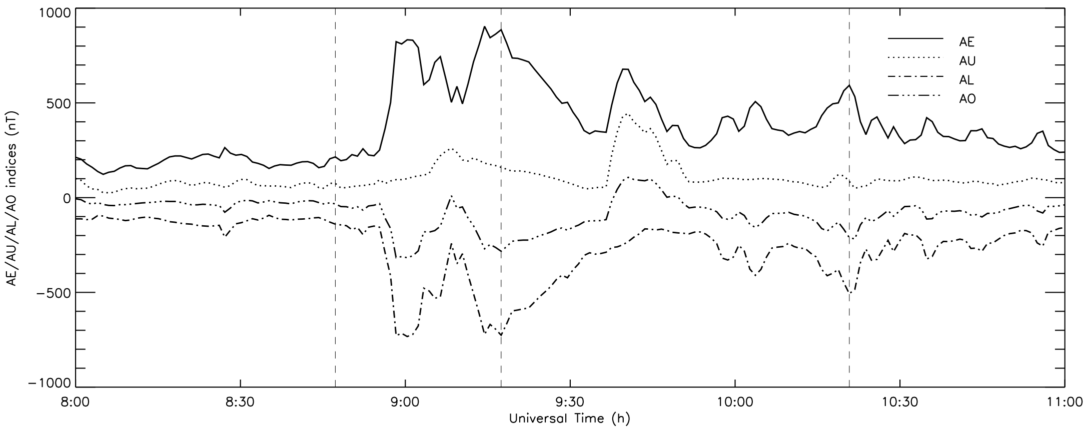

Fig. 7 Time profiles of one-minute AE, AU, AL and AO indices from UTC 8:00 to 11:00 on 2011 Feb 6, adapted from WDC for Geomagnetism, Kyoto. Three reference lines (*dashed lines*) are drawn to represent the start time, peak time and end time, from left to right respectively, the same as Fig. 4.

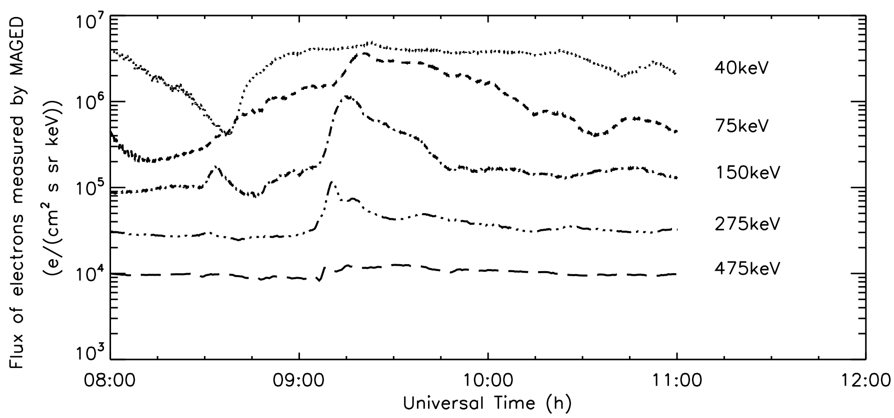

Fig. 8 Time profile of the electron fluxes measured by MAGED onboard *GOES* 15 from UTC 8:00 to 11:00 on 2011 Feb 6. The five curves represent the omni-directional electron flux with the energy channels of 40, 75, 150, 275 and 475 keV, respectively.

reconnection or some other acceleration process. *SDO* and *GOES* 15 were both geosynchronous satellites, with longitudes of 102°W and 89.5°W on 2011 February 6. While the event was going on from 08:48 UT to 10:20 UT, the two satellites were both, coincidentally, turning around at local midnight, operating with the nightside facing the magnetotail within the magnetosphere, where they were vulnerable to the danger of energetic electrons accelerated from magnetic reconnection. Simultaneously, a substorm was also ongoing, making substorm-injections possible to identify from a geosynchronous orbit. The substorm-injection induced electrons will, in bulk, pass by some instruments working at geosynchronous orbit, playing the role of the black sheep in the aliasing of signal and noise. Energetic electron storms occur frequently, especially in years which are not around the maximum of a solar cycle, because coronal holes, which frequently appear in the corona during quiet years, often drive the solar wind up to very high speed. Consequently, nearby space becomes energetic, creating a great volume of accelerated electrons which can damage satellites traveling in scheduled orbits. As a result, for space weather, it is equally essential to consider years when solar activity is lower.

In the end, we will reiterate that this event is a rare case, however it is still worthwhile of study even though it occurs with a low probability. It reminds us that we should carefully examine datasets from times with weaker solar activity and stronger geomagnetic activity, especially in the recovery of a geomagnetic storm. Furthermore, if it were not a real flare, one would think that it might be related to a geophysical event, probably a substorm.

Acknowledgements The authors thank the anonymous referee for his/her valuable suggestions that greatly improved the manuscript. This work is jointly supported by the National Basic Research Program of China (973 Program, Grant 2011CB811406) and the National Natural Science Foundation of China (NSFC, Grant Nos. 11273031, 11473040 and 41231066). Y. Y. owes a great deal to the enlightening opinions offered by

Prof. Leonid Didkovsky that contributed to this work. Dr. Don Woodraska at the LASP/CU team provided the L0D data on our request. Prof. Ronglan Xu gave us some valuable advice on space physics. We acknowledge the XRS/*GOES*, SXI/*GOES*, MAGED/*GOES*, ESP/EVE/*SDO*, SWEPAM/ACE, MAG/ACE and SEM/*SOHO* consortia for usage of the data. The WDC for Geomagnetism, Kyoto is also sincerely acknowledged.

References

Didkovsky, L., Judge, D., Kosovichev, A. G., Wieman, S., & Woods, T. 2011, ApJ, 738, L7

Didkovsky, L., Judge, D., Wieman, S., Woods, T., & Jones, A. 2012, Sol. Phys., 275, 179

Didkovsky, L., Kosovichev, A., Judge, D., Wieman, S., & Woods, T. 2013, Sol. Phys., 287, 171

Du, Z.-L., & Wang, H.-N. 2012, RAA (Research in Astronomy and Astrophysics), 12, 400

Grubb, R. N. 1975, NASA STI/Recon Technical Report N, 76

Hill, S. M., Pizzo, V. J., Balch, C. C., et al. 2005, Sol. Phys., 226, 255

Judge, D. L., McMullin, D. R., Ogawa, H. S., et al. 1998, Sol. Phys., 177, 161

Lean, J. 1987, J. Geophys. Res., 92, 839

Li, C., Sun, L. P., Wang, X. Y., & Dai, Y. 2013, A&A, 556, L2

Pesnell, W. D., Thompson, B. J., & Chamberlin, P. C. 2012, Sol. Phys., 275, 3

Pizzo, V. J., Hill, S. M., Balch, C. C., et al. 2005, Sol. Phys., 226, 283

Rathore, B. S., Gupta, D. C., & Kaushik, S. C. 2015, RAA (Research in Astronomy and Astrophysics), 15, 85

Woods, T. N., Eparvier, F. G., Hock, R., et al. 2012, Sol. Phys., 275, 115